Supporting Information: Elucidating Correlated Defects in Metal Organic Frameworks Using Theory-Guided Inelastic Neutron Scattering Spectroscopy

Lucas S. R. Cavalcante,[†] Makena A. Dettmann,[†] Tyler Sours,[†] Dong Yang,[†] Luke L. Daemen,[‡] Bruce C. Gates,[†] Ambarish R. Kulkarni,[*,†] and Adam J. Moulé[*,†]

[†]*Department of Chemical Engineering, University of California, Davis, CA, 95616, USA*

[‡]*Neutron Scattering Division, Oak Ridge National Laboratory, Oak Ridge, Tennessee 37831, United States*

E-mail: arkulkarni@ucdavis.edu; amoule@ucdavis.edu

Sample preparation

Synthesis of UiO-66 with Modulators. $ZrCl_4$ (0.120 g, 0.515 mmol) and the modulators (1.00 mL acetic acid (AA) or 1.18 mL trifluoroacetic acid (TFA)) were dissolved in 20 mL of DMF in an 8-dram vial using ultrasound for 5 min. The mol ratio of modulators to Zr were both 30. 0.086 g of the linker precursor (benzene-1,4-dicarboxylic acid or a functionalized BDC linker precursor) was then added to the solution and dissolved by ultrasound for 15 min. The vials were kept under static conditions in a preheated oven at 393 K for 24 h. MOF precipitates formed, and they were isolated by centrifugation after cooling to room temperature. The solids were washed with DMF (30 mL) three times in a day to remove unreacted precursors and with acetone (30 mL) six times in 2 days to remove DMF. Then, the powder was dried at room temperature and activated at 393 K under vacuum for 18 h prior to characterization.

INS experiment details

The neutron vibrational spectra were collected at the VISION beam line (Spallation Neutron Source, Oak Ridge National Laboratory). VISION is an inverted geometry spectrometer with a resolution of 1-1.5% over the -2 $<$ E $<$ 1000 meV dynamic range. It measures neutron incident energy with the time-of-flight method. The final neutron energy is fixed and selected by Bragg reflection on a series of curved, pyrolytic graphite analyzers. The samples were placed in cylindrical vanadium sample holders (8 mm diam. x 50 mm height). The samples were inserted in a top-loading, closed-cycle refrigerator and cooled to 5 K before data collection. It took approximately 2 hours to collect each spectrum. An empty sample holder was also measured, and the corresponding signal was subtracted from all the data sets to remove beam-related background associated with scattering from aluminum windows, heat shield, vacuum shroud, and sample holder. Slits were used to reduce the beam size to illuminate only the sample during the experiment.

INS simulation details

All the simulations were accomplished using the Vienna Ab initio Simulation Package (VASP) with projector augmented-wave pseudo-potentials[1,2] and the Perdew-Burke-Ernzerhof (PBE) density functional[3] with DFT-D3 vdW corrections.[4] The atomic positions and lattice parameters were optimized considering a energy cutoff of 520 meV and force criteria of 0.01 eV/Å. In order to calculate the phonon modes, the supercell displacement method was used with a simulation box of the same size as the original and forces being calculated at the gamma point. Finally, oclimax[5] used the phonon modes with a q-point sampling of 8 x 8 x 8 to calculate the INS spectrum.

INS comparison to optical spectroscopy methods

In a simple example, we demonstrate the advantages of INS over optical spectroscopy methods with a organic electronic material (TIPS-PN) as the studied system. In Fig. 1, INS demonstrates a much wider energy spectrum compared to RAMAN and FTIR. Furthermore, since INS can sample the complete Brillouin zone, it presents a much higher density of peaks in the whole spectrum.

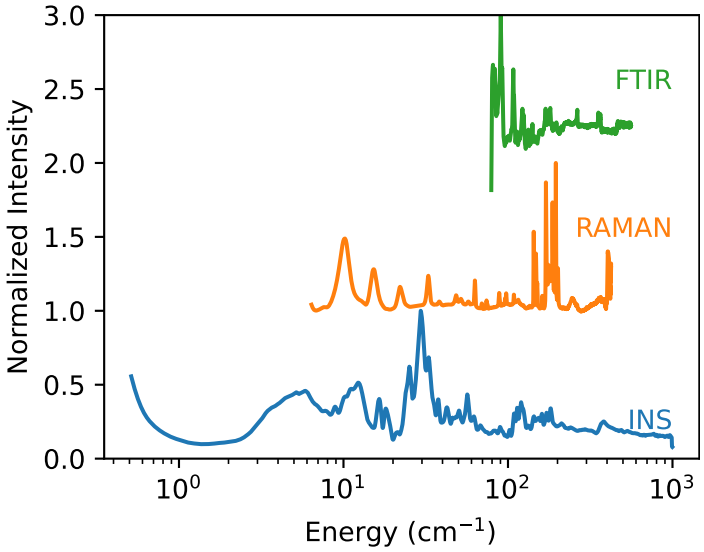

Figure 1: Spectra comparison between INS, RAMAN and FTIR for organic electronic material (TIPS-PN). The energy axis in the log scale demonstrates the much broader energy range accomplished with INS, besides the much higher density of peaks in the whole spectrum.

Combined simulation and experiment approach

The overall approach for fingerprinting defects in the UiO-66 MOF with theory-guided Inelastic Neutron Scattering (INS) experiments is given in Fig. 2. The flowchart shows the iterative method of simulating INS of a structure taken from a library of possible defect structures. Depending on the agreement with the experiment, another simulation can be done with a different configuration of defects. The library of defects was constructed considering possible connectivity defects (missing linkers and missing nodes) and/or possible chemical defects derived from the synthesis process (node ligands such as formates and acetates).

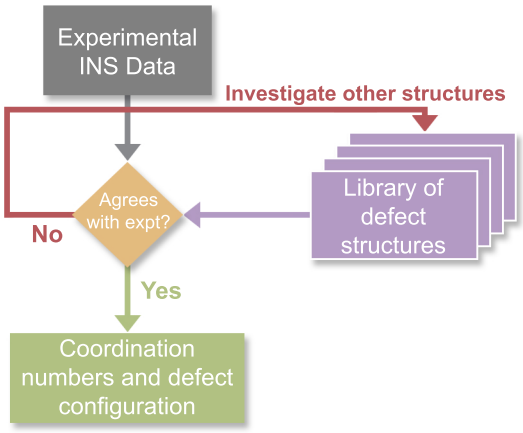

Figure 2: Flowchart summarizing overall approach to predict INS from a library of candidate defect structures to be compared with the experimental measurements.

FCU simulation

The detailed comparison between experimental INS from the UiO-66-AA sample and simulation of the fcu model up to 5000 cm^{-1} is given in Fig. 4

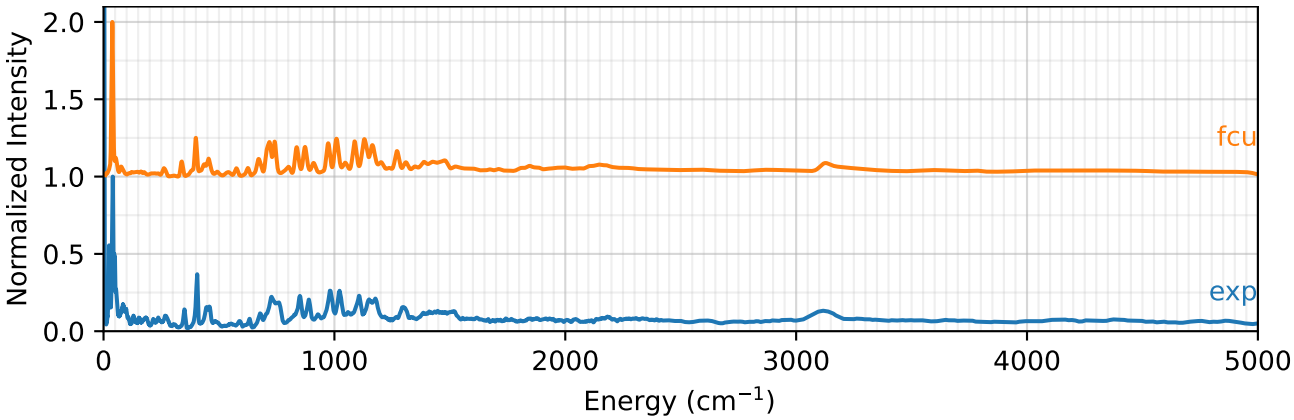

Figure 3: INS spectra up to 5000 cm^{-1} for simulated fcu topology (orange) in comparison to experiment modulated with CH_3 (blue).

Correlation

In order to quantitatively characterize the degree to which each simulation agrees with the experiment, a correlation-based analysis method was employed. An experimental INS spec-

trum from the VISION spectrometer contains a higher density of points in the low energy and a lower density of points in the high energy. In contrast, a simulated spectrum contains equally spaced points across all energies. To account for this difference, the experimental spectrum is down-sampled by finding the nearest experimental point in energy to the regularly-spaced simulated spectrum. This process does not meaningfully change the experimental spectrum. Next, the correlation is computed between each simulated spectrum and the experimental spectrum. Correlation is used because it captures similarity in a way that accounts for peak shifts in energy and intensity unlike simple subtraction. The correlation coefficient is defined by

$$r = \frac{n\left(\sum(I_{exp}I_{sim})\right) - \left(\sum I_{exp}\right)\left(\sum I_{sim}\right)}{\sqrt{\left[n\left(\sum I_{exp}^2\right) - \left(\sum I_{exp}\right)^2\right]\left[n\left(\sum I_{sim}^2\right) - \left(\sum I_{sim}\right)^2\right]}} \tag{1}$$

where r is the correlation coefficient, n is the number of points, I_{exp} are the intensities of each experimental point, and I_{sim} are the intensities of each simulated point.

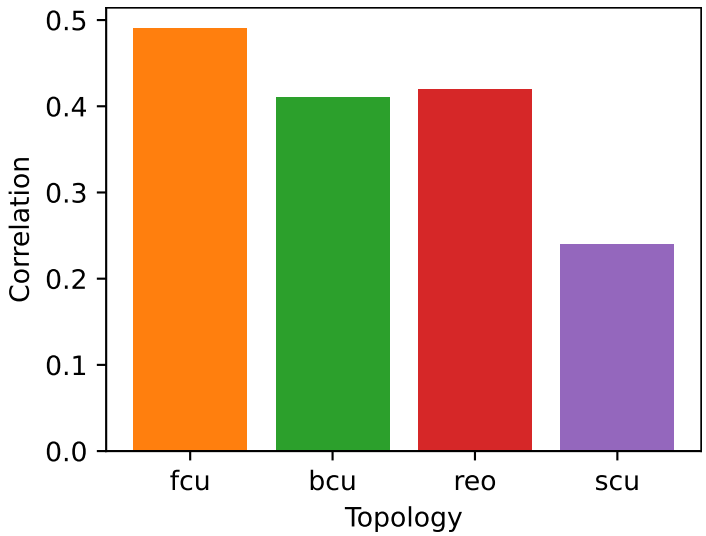

Figure 4: Correlation between the INS experimental spectrum and the DFT simulated spectra produced by each topology.

Analysis of the formate contribution to the INS spectra

Incoherent INS obeys the following scattering law, which is a response function of the vibrational modes due to a transferred momentum from the neutron ($\mathbf{Q}$) at a frequency (ω):[5]

$$\begin{aligned} S_{inc\pm1}(\mathbf{Q},\omega) = \sum_d \frac{1}{2M_d}\left\{\overline{b_d^2} - (\overline{b_d})^2\right\}\exp(-2W_d) \\ \times\frac{|(\mathbf{Q}\cdot\mathbf{e}_{ds})|^2}{\omega_s}\left(n_s+\frac{1}{2}\pm\frac{1}{2}\right)\delta(\omega\mp\omega_s), \end{aligned} \tag{2}$$

where ω_s is the frequency of the phonon mode s, $\mathbf{e}_{ds}$ is the polarization vector, $\overline{b_d}$, M_d, and W_d are respectively the neutron scattering length, the atomic mass, and the Debye-Waller factor. We call $\overline{b_d^2} - (\overline{b_d})^2$ as the incoherent cross-section. Therefore, the INS is given by the sum over all the atomic contributions.

In order to determine the origin of the peaks around 250 cm^{-1} and 1350 cm^{-1} of Fig. 1 of the main text, we can isolate the formate contributions to INS from all the other modes. This is possible by setting the atomic cross-section of the formate atoms to zero (no formate contributions) when calculating the INS spectrum. This was done for the bcu (Fig. 5), reo (Fig. 6) and scu topologies (Fig. 7). The figures show that the mentioned peaks only appear when the contributions of formate groups are considered. Furthermore, as we increase the number of formates going from bcu and reo (4 formates per node), to scu (4/8 formates/node) the peak intensities increase.

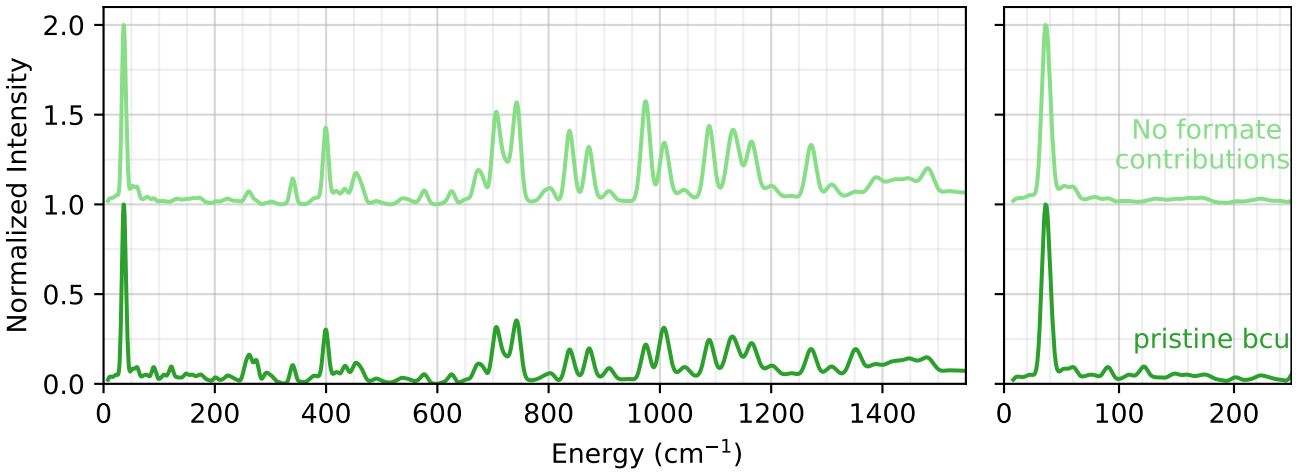

Figure 5: INS spectrum comparison of the bcu MOF, where the defective sites are capped by formates, with (dark green) and without (light green) formate groups contributions.

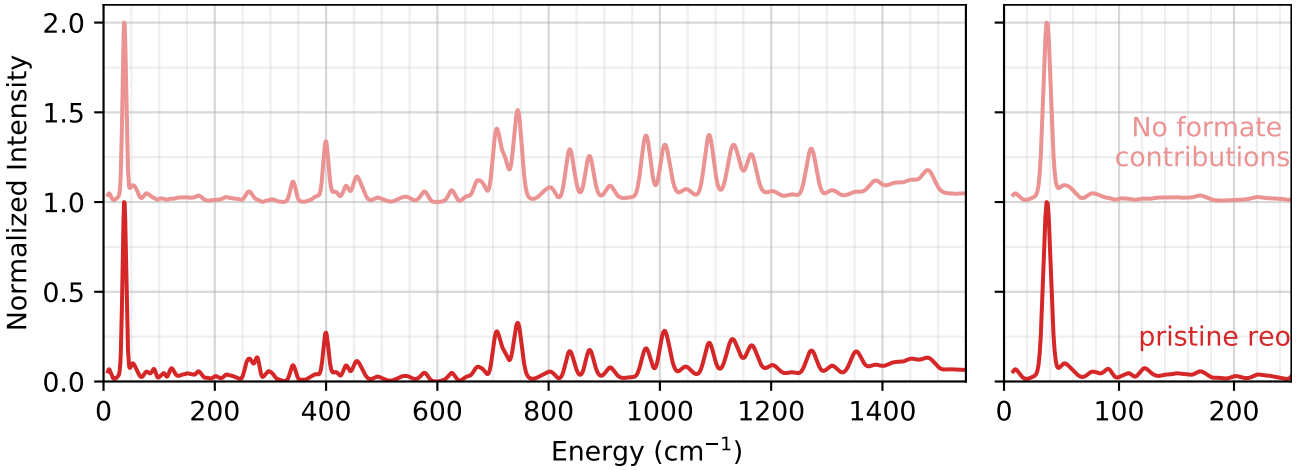

Figure 6: INS spectrum comparison of the reo MOF, where the defective sites are capped by formates, with (dark red) and without (light red) formate groups contributions.

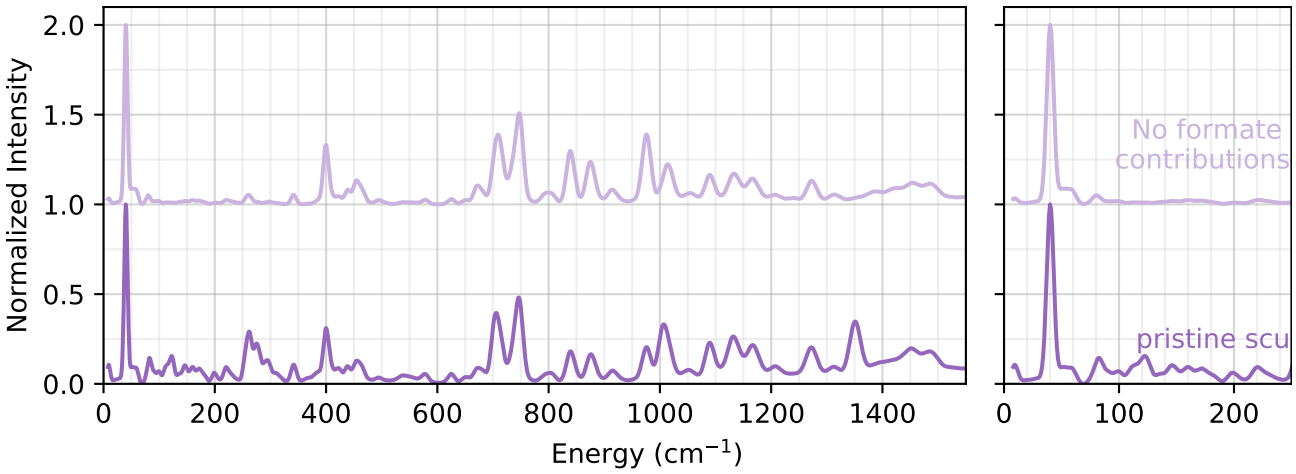

Figure 7: INS spectrum comparison of the scu MOF, where the defective sites are capped by formates, with (dark purple) and without (light purple) formate groups contributions.

Mode analysis of peaks A, B, and C

The simulations of four different variations of the bcu defective topology present similar peaks in the fingerprint region to peaks A, B, and C of the experiment. The atomic motions related to the double peak a1 and a2 in the bcu topology where all defective sites are saturated with acetate groups is shown in Files *bcu-4A_a1.gif* and *bcu-4A_a2.gif*. In this case, each peak is related to the motions of one diagonal of defects. In Files *bcu-2A2F_a.gif* and *bcu-2A2F_b.gif*, the atomic motions related to peaks a and b are presented for the system that contains one diagonal of acetate groups and another with formate groups. In this case, the motions of peak a are isolated motions of acetate groups, while peak b is a combination of linkers and acetates groups in a "breathing" motion. Finally, Files *bcu-2A2F-2F2A_b1.gif*, *bcu-2A2F-2F2A_b2.gif* and *bcu-2A2F-2F2A_c.gif* describe the vibrations in the system with a unit cell containing two clusters where each is passivated with two different diagonals of acetates and formates groups. The doublet b (b1 and b2) is related to motions of neighbors acetates coupled to the framework. Furthermore, the motions derived from peak c involve all the acetates in the system coupled to the framework.

References

(1) Blöchl, P. E. Projector augmented-wave method. *Physical Review B* **1994**, *50*, 17953.

(2) Kresse, G.; Joubert, D. From ultrasoft pseudopotentials to the projector augmented-wave method. *Physical Review B* **1999**, *59*, 1758.

(3) Perdew, J. P.; Burke, K.; Ernzerhof, M. Generalized Gradient Approximation Made Simple. *Physical Review Letters* **1996**, *77*, 3865.

(4) Grimme, S.; Antony, J.; Ehrlich, S.; Krieg, H. A consistent and accurate ab initio parametrization of density functional dispersion correction (DFT-D) for the 94 elements H-Pu. *The Journal of Chemical Physics* **2010**, *132*, 154104.

(5) Cheng, Y. Q.; Daemen, L. L.; Kolesnikov, A. I.; Ramirez-Cuesta, A. J. Simulation of Inelastic Neutron Scattering Spectra Using OCLIMAX. *Journal of Chemical Theory and Computation* **2019**, *15*, 1974–1982.